The Prospects for Mechanical Ratcheting of Bulk Metallic Glasses

Wendelin J. Wright[1], R.H. Dauskardt[2], and W.D. Nix[2]
[1]Lawrence Livermore National Laboratory, University of California, Livermore, CA 94550
[2]Department of Materials Science and Engineering, Stanford University, Stanford, CA 94305

ABSTRACT

The major mechanical shortcoming of metallic glasses is their limited ductility at room temperature. Monolithic metallic glasses sustain only a few percent plastic strain when subjected to uniaxial compression and essentially no plastic strain under tension. Here we describe a room temperature deformation process that may have the potential to overcome the limited ductility of monolithic metallic glasses and achieve large plastic strains. By subjecting a metallic glass sample to cyclic torsion, the glass is brought to the yield surface; the superposition of a small uniaxial stress (much smaller than the yield stress) should then produce increments in plastic strain along the tensile axis. This accumulation of strain during cyclic loading, commonly known as ratcheting, has been extensively investigated in stainless and carbon steel alloys, but has not been previously studied in metallic glasses. We have successfully demonstrated the application of this ratcheting technique of cyclic torsion with superimposed tension for polycrystalline Ti–6Al–4V. Our stability analyses indicate that the plastic deformation of materials exhibiting elastic–perfectly plastic constitutive behavior such as metallic glasses should be stable under cyclic torsion, however, results obtained thus far are inconclusive.

STABILITY ANALYSIS

The ratcheting process proposed here for metallic glasses will achieve large plastic strains only if the torsional deformation that is imposed is stable after yielding has occurred. For this reason, we now consider the relationship between the applied torque and the angle of twist after yielding has commenced.

During pure torsional deformation under rotational control, one end of a cylindrical sample of radius R and length L is twisted by an angle θ relative to the fixed end. The shear strain γ is given by $\gamma = \frac{r\theta}{L}$, where r is the radius at which the strain is to be evaluated. The shear stress τ in the elastic core is computed as $\tau = \mu\,\gamma$, where μ is the shear modulus of the material. Thus $\tau = \frac{\mu\theta}{L} r$, and the maximum shear stress occurs at the surface of the cylinder where $r = R$.

The applied torque in a sample subjected to pure shear is found by integrating

$$T = \int_0^R \left(\tau\, 2\pi r\, dr\right) r. \tag{1}$$

The applied torque T_y at which yielding commences is calculated by substituting for τ with $\theta = \theta_y$, the critical angle of twist for yielding, and performing the integration,

$$T_y = \int_0^R \left(\frac{\mu\,\theta_y}{L}\, r\, 2\pi r\, dr \right) r = 2\pi \frac{\mu\,\theta_y}{L} \int_0^R r^3\, dr = \frac{\pi}{2} \frac{\mu\,\theta_y}{L} R^4 = \frac{\pi}{2} \tau_y R^3, \tag{2}$$

where the shear yield strength is given by $\tau_y = \frac{\mu\,\theta_y}{L} R$. Assuming elastic–perfectly plastic behavior for metallic glasses, the shear stress τ increases linearly from the center of the cylinder to the elastic–plastic boundary, which will be denoted as the radius where $r = a$, and is equal to τ_y for $r > a$. The location of the elastic–plastic boundary is given by

$$\tau\,(r = a) = \tau_y = \frac{\mu\,\theta}{L} a, \tag{3}$$

such that

$$a = \frac{\tau_y\, L}{\mu\,\theta}. \tag{4}$$

At the surface of the cylinder where the material first yields,

$$\tau_y = \frac{\mu\,\theta_y}{L} R. \tag{5}$$

Substituting Equation 5 for τ_y in Equation 4, it is convenient to write

$$a = \frac{\theta_y}{\theta} R. \tag{6}$$

Thus when $\theta = \theta_y$, $a = R$, and when $\theta > \theta_y$, $a < R$. The applied torque T after yielding commences is given by

$$T = \int_0^a \left(\tau\, 2\pi r\, dr\right) r + \int_a^R \left(\tau_y\, 2\pi r\, dr\right) r. \tag{7}$$

Substituting for τ in Equation 7 and performing the integration,

$$T = \frac{\pi}{2}\frac{\mu\,\theta}{L} a^4 + \frac{2\pi}{3}\tau_y\left(R^3 - a^3\right). \tag{8}$$

Substituting $\frac{\mu}{L} = \frac{\tau_y}{\theta_y\, R}$ from Equation 5 and $a = \frac{\theta_y}{\theta} R$ from Equation 6, we find

$$T = \frac{\pi}{2}\tau_y\, R^3\left[\left(\frac{\theta_y}{\theta}\right)^3 + \frac{4}{3} - \frac{4}{3}\left(\frac{\theta_y}{\theta}\right)^3\right] = \frac{\pi}{2}\tau_y\, R^3\left[\frac{4}{3} - \frac{1}{3}\left(\frac{\theta_y}{\theta}\right)^3\right]. \tag{9}$$

From Equation 2, $T_y = \frac{\pi}{2}\tau_y\, R^3$, such that

$$T = T_y\left[\frac{4}{3} - \frac{1}{3}\left(\frac{\theta_y}{\theta}\right)^3\right]. \tag{10}$$

A plot of the applied torque T versus the angle of twist θ for pure shear is shown in Figure 1(a). Thus we see that if the elastic–perfectly plastic constitutive law holds, the applied torque continues to increase after yielding, and stable torsional deformation occurs.

Yielding is characterized by the initiation and propagation of shear bands. It is possible that the shear bands that form in the plastic zone at the surface of the cylinder during yielding transform to cracks [1]. In this case, the plastic zone would not be able to support the applied shear stress, and the applied torque would decrease with increasing θ. It is necessary to calculate the relationship between the torque T and the angle of twist θ after yielding if cracking occurs in order to determine whether the torsional deformation would be stable. If the plastic zone supports none of the shear stress, then when the material has yielded and $\theta > \theta_y$, the applied

torque would be supported only by the elastic core. In this case, the second term of Equation 7 is equal to zero, and the applied torque is given by

$$T = 2\pi \frac{\mu\,\theta}{L}\int_0^a r^3\,dr = \frac{\pi}{2}\frac{\mu\,\theta}{L}a^4. \tag{11}$$

Substituting $\frac{\mu}{L} = \frac{\tau_y}{\theta_y\,R}$ from Equation 5, $a = \frac{\theta_y}{\theta}R$ from Equation 6, and $T_y = \frac{\pi}{2}\tau_y\,R^3$ from Equation 2,

$$T = T_y\left(\frac{\theta_y}{\theta}\right)^3. \tag{12}$$

Equation 12 is valid only for $\theta > \theta_y$. The applied torque T as a function of the angle of twist θ is shown in Figure 1(b) for the case in which the shear bands that form after yielding in pure shear transform to cracks and the plastic zone does not support any of the applied torque. In contrast to the results of Figure 1(a), the applied torque decreases when $\theta > \theta_y$.

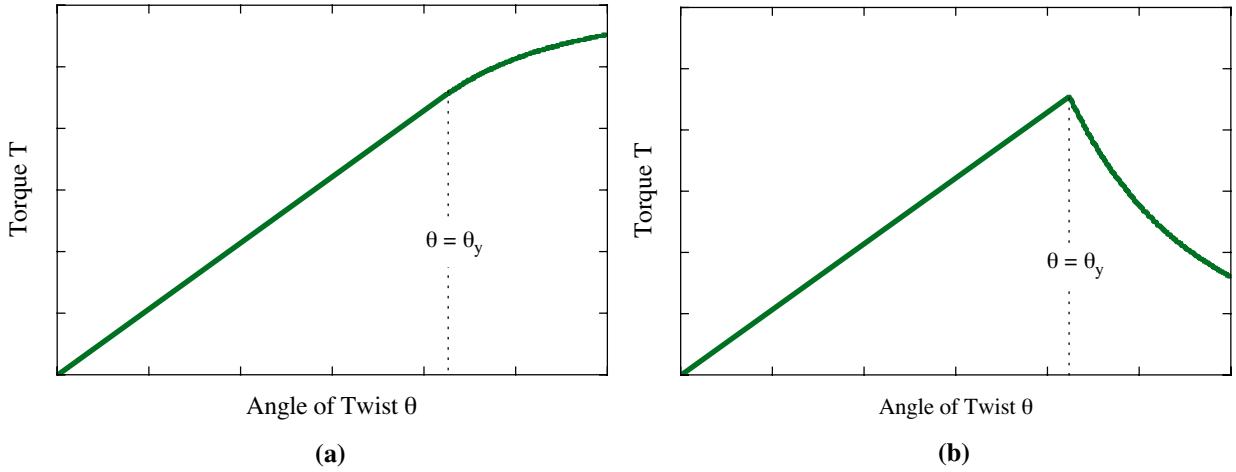

Figure 1. (a) A plot of the applied torque T versus the angle of twist θ for pure shear assuming elastic–perfectly plastic material behavior. **(b)** A plot of the applied torque T versus the angle of twist θ for pure shear assuming that the shear bands that form after yielding transform to cracks and the plastic zone does not support any of the applied torque.

If the shear bands that form upon yielding transform to cracks when $\theta > \theta_y$, the torque needed to enforce continued torsional deformation would fall with increasing torsional displacement according to Equation 12. This expression for the applied torque T assumes that the testing machine twisting the sample is perfectly rigid. This deformation would be stable only if the testing system is stiff enough to twist the sample under these conditions. We consider twisting the sample with a testing machine having a finite torsional stiffness k_m, which can be written $k_m = \frac{dT}{d\theta_m}$. For such a system, the total torsional displacement can be expressed as $\theta_{total} = \theta + \theta_m$, where θ is the twist of the sample and θ_m is the twist accommodated by the machine. If the sample suddenly twists by a small amount $\delta\theta$ under displacement control, then

$$\delta\theta_{total} = 0 = \delta\theta + \delta\theta_m, \tag{13}$$

and

$$\delta\theta_m = -\delta\theta . \tag{14}$$

This causes the applied torque on the sample to change by

$$\delta T = k_m \delta\theta_m = -k_m \delta\theta . \tag{15}$$

The torsional resistance of the sample also changes. Following Equation 12, the torque T_{flow} required to maintain the shear stress at τ_y at the elastic–plastic boundary for the case of a testing machine with a finite torsional stiffness is given by $T_{flow} = T_y \left(\frac{\theta_y}{\theta} \right)^3$, and thus the torsional resistance of the sample changes by

$$\delta T_{flow} = -3k_s^i \left(\frac{\theta_y}{\theta} \right)^4 \delta\theta , \tag{16}$$

where $k_s^i = \frac{T_y}{\theta_y}$ is the initial torsional stiffness of the sample. If δT is more negative than δT_{flow}, then the torsional flow process is stable. For such stable flow, the applied torque will have fallen below the torsional resistance. Thus the condition for stable flow is

$$\delta T < \delta T_{flow} . \tag{17}$$

Substituting for δT and δT_{flow} from Equations 15 and 16,

$$-k_m \delta\theta < -3k_s^i \left(\frac{\theta_y}{\theta} \right)^4 \delta\theta , \tag{18}$$

and simplifying,

$$k_m > 3k_s^i \left(\frac{\theta_y}{\theta} \right)^4 . \tag{19}$$

If this condition is met when $\theta = \theta_y$, then it will also be satisfied for $\theta > \theta_y$ since the term on the right in Equation 19 decreases with increasing θ. Thus the absolute condition for stable flow can be written

$$k_m > 3k_s^i . \tag{20}$$

For unstable flow the torsional resistance falls more quickly that the applied torque so that equilibrium will never be re–established.

EXPERIMENTAL RESULTS

Ratcheting of Ti–6Al–4V

According to the stability analysis presented above for an elastic–perfectly plastic material, it should be expected that torsional deformation of an elastic–plastic material that exhibits work hardening such as polycrystalline Ti–6Al–4V would also be stable. An axial–torsional MTS servohydraulic machine with hydraulic sample grips was used to impose multi–axial deformation on polycrystalline samples of Ti–6Al–4V. A load cell with 111 kN axial capacity and 1410 N•m torsional capacity was used. The load cell was calibrated to operate in the ±9 kN (±2000 lb) and ±115 N•m (1000 in•lb) ranges. Displacements were measured by linear and rotational variable differential transformers attached to the actuator. Cylindrical dogbone specimens with radii of 2 mm and gage lengths of 20 mm were used. The yield strength of the

Ti–6Al–4V was determined to be 1040 MPa from uniaxial tension testing. To perform the ratcheting experiment, the Ti–6Al–4V was loaded to a uniaxial tensile stress of 530 MPa at a rate of 20 N/s. The axial load was maintained under load control during the subsequent torsional cycling. Under load control, the displacement of the sample is not constrained in the axial direction. The sample was then twisted under rotational control (±12) with a sinusoidal waveform at a rate of 0.05 /second until the sample yielded in shear at surface shear stresses of 650 MPa. The axial displacement as a function of the applied torque is shown in Figure 2. Note that although the stress in the axial direction is not large enough to cause yielding, a permanent displacement in the axial direction of 0.32 mm is retained after the sample is unloaded. This displacement corresponds to a plastic strain of 1.6% and demonstrates the success of the ratcheting technique.

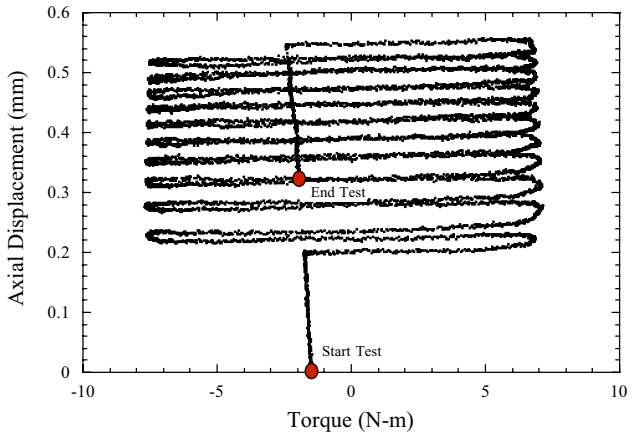

Figure 2. Axial displacement versus torque for Ti–6Al–4V.

Ratcheting of $Zr_{41.2}Ti_{13.8}Cu_{12.5}Ni_{10.0}Be_{22.5}$

Similar ratcheting experiments were performed on samples of the alloy $Zr_{41.2}Ti_{13.8}Cu_{12.5}Ni_{10.0}Be_{22.5}$ (Vitreloy 1). Cylindrical dogbone specimens with radii of 1.5 mm and gage lengths of 20 mm were electrode discharge machined (using low power and water cooling to prevent crystallization) from cast rods (12.5 mm diameter) provided by Liquid Metal Technologies, Inc. A uniaxial tension stress of 920 MPa was imposed and maintained constant under load control while the sample was cycled in shear. As with the titanium samples, this stress is nominally half of the tensile yield strength (1.9 GPa for Vitreloy 1) [2]. The sample was then cycled in torsion (0.05 /second under rotational control) to surface shear stresses of nominally 1000 MPa. The shear modulus was determined to be 31 GPa, in close agreement with the previously reported value of 34 GPa for the same alloy [2]. No corrections for the finite torsional stiffness of the machine were performed in order to determine the shear modulus of the material, indicating that the machine is exceptionally stiff in torsion and meets the stability condition expressed in Equation 20. Thus we should expect stable torsional deformation to occur during ratcheting of Vitreloy 1. The sample failed abruptly during elastic loading after several cycles, however, at a surface shear stress of 870 MPa even though surface shear stresses as large as 925 MPa were sustained earlier in the test, indicating that flaws in the samples may have precipitated the failure. Figure 3(a) is a plot of axial displacement versus torque for $Zr_{41.2}Ti_{13.8}Cu_{12.5}Ni_{10.0}Be_{22.5}$ that, in contrast to Figure 2, clearly indicates that the ratcheting technique was not successful in this case.

Figure 3(b) is a scanning electron micrograph depicting the surface damage caused by the electrode discharge machining process. In this experiment, these flaws have characteristic sizes on the order of tenths of millimeters. The cylindrical gage sections of the ratcheting samples were not polished after machining. Having observed these flaws, it is not surprising that premature failure occurred. Thus the results of the ratcheting experiments on Vitreloy 1 are inconclusive. The stability analysis for torsional deformation indicates that it should be possible to achieve substantial plastic strains through a ratcheting process for a metallic glass with elastic–perfectly plastic constitutive behavior. The quality of the surface finish of the samples used in these experiments, however, was too poor to yield meaningful results. Ideally samples should be cast in the final form for the test geometry if these experiments are to be performed again.

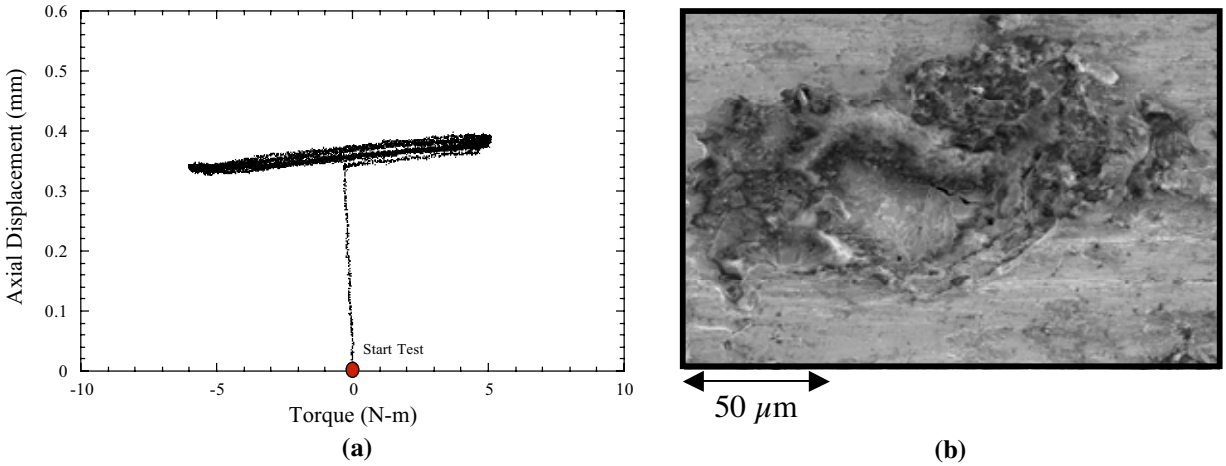

Figure 3. (a) Axial displacement versus torque for $Zr_{41.2}Ti_{13.8}Cu_{12.5}Ni_{10.0}Be_{22.5}$. **(b)** A scanning electron micrograph of one of the flaws on the surface of the sample due to the machining process.

ACKNOWLEDGEMENTS

The work at Stanford University was sponsored by the Structural Amorphous Metals Program of the Defense Advanced Research Projects Agency (DARPA), under ARO Contract No. DAAD19-01-1-0525. Samples were provided by Liquid Metal Technologies, Inc. The technical assistance of S.J. DeTeresa, G.J. Larsen, M.M. LeBlanc, and R.J. Sanchez at LLNL is greatly appreciated. This work was performed under the auspices of the U.S. Department of Energy by the University of California, Lawrence Livermore National Laboratory under Contract W-7405-Eng-48.

REFERENCES

1. R.D. Conner, W.L. Johnson, N.E. Paton, and W.D. Nix, J. Appl. Phys. **94** 904 (2003).
2. R.D. Conner, A.J. Rosakis, W.L. Johnson, and D.M. Owen, Scripta Mater. **37** 1373 (1997).